ARTICLE | Article in Press

Optimizing metro and BRT transfer design in Isfahan using passenger generalized cost and ant colony optimization

Navid Nakhaie · Ali Naderan · Shahriar Afandizadeh Zargari · Hooman Rahimi

Received: 28 May 2026 / Accepted: 28 September 2026
© The Author(s) 2026

Abstract

This study presents a revised framework for screening and optimizing local Metro and BRT transfer connections in Isfahan using a state-separated passenger network, fixed-OD evaluation, explicit transfer screening, and ant-colony-based search. The formulation prevents implicit intermodal switching and holds the OD matrix constant between baseline and intervention networks, thereby separating modeled network-design effects from demand regeneration. Because the available empirical demand information does not provide a complete observed spatial OD matrix, the gravity deterrence coefficient is treated as a sensitivity parameter rather than as an empirically calibrated behavioral coefficient. Coordinate and network screening retained 29 feasible transfer candidates. Candidate 22, a 249.2 m pedestrian connection, produced the largest modeled improvement in the central case. System passenger generalized cost decreased from 6,265,519.636 to 6,258,241.797 passenger-min, a reduction of 7,277.839 passenger-min (0.116157%). Exhaustive evaluation of all 406 candidate pairs and targeted triple screening found no additional benefit beyond the best single link. I-ACO, standard ACO, and greedy search identified the same one-link solution, although the fast benchmark does not establish statistical superiority of any stochastic algorithm. Given the small system-wide effect and limitations in observed OD validation, route-choice behavior, and service-parameter calibration, the result is interpreted as a localized model-based screening outcome that requires empirical and site-level validation before implementation.

Keywords Metro–BRT integration · Transfer design · Multimodal network · Generalized cost · Gravity model

Introduction

In contemporary transport planning for historic cities, the central question is no longer whether a mass public transport system is needed, but how such a system should be designed to reconcile mobility, sustainability and heritage protection. Isfahan illustrates this tension with particular clarity: rapid growth in car ownership and dispersed travel patterns coexist with a finely grained traditional street network and sensitive cultural landscapes. Recent extensions of the metro and BRT network offer a rare window of opportunity to reshape the structure of

This Article in Press is shared early to give you faster access to new research. It is citable and carries a permanent DOI. The final edited version will replace it automatically.

Published online: 13 October 2026

scientific reports

daily trips, yet the way these lines are aligned, connected and sequenced will lock in environmental, social and spatial outcomes for decades to come. Over the past decade, sustainable urban mobility has moved from a normative aspiration to a central requirement for climate policy, air-quality management and social equity in cities, particularly in the Global South. A substantial share of urban energy use and greenhouse gas (GHG) emissions is associated with passenger transport, while congestion and local air pollutants continue to undermine live-ability and public health. Recent work on urban transport sustainability has therefore advanced indicator-based frameworks and composite indices that assess performance across environmental, economic and social dimensions in a more systematic way [Nitwal et al., 2025[1]. Nevertheless, several reviews point out that existing indices often suffer from methodological inconsistencies, sensitivity to weighting schemes and limited applicability to concrete investment decisions [Buzási and Csete, 2015; Ayadi et al.,2024].

A first strand of the literature develops sustainable transport indicators and composite indices at the city or corridor scale. Nitwal[2], for example, proposes a composite index based on 29 sustainable transport indicators to evaluate policy interventions and track progress toward transport-related Sustainable Development Goals. Reisi[1] derive and evaluate transport sustainability indicators using an Urban Analytics Data Infrastructure, illustrating how integrated data platforms can support cross-city benchmarking and scenario analysis. Other contributions focus on indicator design and normalization rules for specific regional contexts or for planning tools such as the Sustainable Transport Planning Index (STPI) and related multi-dimensional indices for public transport systems[3]. Despite their value, these frameworks typically regard the public transport network configuration as exogenous: the indices are applied to existing or plan-based systems, rather than used to guide the endogenous design of mass public transport networks[4]; Antczak, 2023]

A second strand uses multi-criteria decision-making (MCDM) techniques—most notably the Analytic Hierarchy Process (AHP) and TOPSIS—to structure complex transport planning problems and to capture expert and stakeholder preferences. Applications range from sustainable transport planning indices that weight environmental, economic and social criteria, to city-level decision-support tools for prioritizing sustainable urban transport strategies5. These approaches show that MCDM can effectively translate qualitative preferences into quantitative trade-offs, but they are usually applied as evaluation and ranking tools over a limited set of pre-defined policy options or corridors. In most cases, the geometry and topology of the underlying public transport network remain fixed, and MCDM outputs do not directly drive systematic network redesign[6]; Nnene et al.[7].

The case of Isfahan has received particular attention in the sustainability literature. An urban sustainable transportation indicator system was developed for Isfahan, using system dynamics to evaluate alternative policy combinations and showing that transit network development is one of the most effective levers to improve transport sustainability[8]. At a finer spatial scale, the sustainability of transport infrastructure projects assessed in the Azadi district of Isfahan, demonstrating how capacity-oriented projects can negatively affect environmental and social indicators in historic neighborhoods if sustainability criteria are not fully integrated[9]. Complementary ecological footprint studies estimate that Isfahan operates under a substantial ecological deficit, with per capita ecological footprints—driven in part by transport—significantly exceeding local bio-capacity[10]; Keshtkar & Sayahnia[11]]. These Isfahan-specific works highlight both the urgency of transport de-carbonization and the particular vulnerability of historic urban fabrics, but they treat the mass public transport network itself as given. Several studies employ MCDM for public transport decision-making in Isfahan. applied AHP and clustering were applied in [Salavati et al., 2016] to prioritize public transport corridors, defining criteria that reflect local demand, existing services and network conditions. In subsequent work, an AHP–TOPSIS framework was used with sustainability indicators in [Salavati et al., 2016] to compare public transport alternatives (metro, BRT, bus) for Isfahan, revealing the sensitivity of mode choice to environmental and social criteria. Other local studies use AHP, TOPSIS and related methods for ranking infrastructure or technology options in the Isfahan region, confirming the suitability of MCDM for structuring multi-criteria decisions in this context[12]. However, these contributions operate at the level of mode or corridor selection, not at the level of endogenously designing an integrated metro–BRT network that maximizes a composite sustainability objective under explicit constraints. A third, largely parallel

strand of research addresses the transit network design problem (TNDP) and relies heavily on metaheuristic algorithms. Reviews of TNDP methods document extensive use of Genetic Algorithms, Simulated Annealing, Tabu Search, Ant Colony Optimization (ACO) and hybrid metaheuristics to design routes, set frequencies and coordinate schedules in complex transit systems [Johar et al., 2016]. Metaheuristic optimization with agent-based simulation were combined in[13] to design transit networks in a large-scale setting, emphasizing the need for flexible search strategies in the face of nonconvex objective functions and multiple constraints. A self-regulated ACO algorithm for designing capacity-constrained transport networks was developed in [Duran-Micco & Vansteenwegen[14]] showing that ant-based heuristics can efficiently optimize route structures and frequencies under demand, capacity and performance constraints. Within this metaheuristic literature, ACO is particularly attractive for route-based design problems that can be represented as paths on graphs. ACO variants have been used for bus transit network design, route optimization and infrastructure planning, sometimes in combination with GIS-based analysis or multi-objective formulations [Ahmadi, 2020]. Recent work proposes modified ACO approaches to evaluate new public transport infrastructure sections and optimize route structures with respect to multiple performance criteria [z Korzeń & Kruszyna[15]]. However, the objective functions in most ACO-based TNDP studies are limited to generalized travel cost, passenger time or operator cost, occasionally complemented by simple measures of emissions or coverage. The multi-dimensional sustainability context of historic cities, including explicit environmental, social and heritage-related constraints, is rarely embedded in the core optimization loop[16]. A further relevant body of work concerns the ASIF framework (Activity–Structure–Intensity–Fuel) for transport emission accounting and scenario analysis. Development banks and international agencies have used ASIF-based approaches to assess transport CO_2 emissions from projects and national policies, decomposing changes into mobility demand, modal structure, energy intensity and fuel carbon content [Asian Development Bank, 2009; Liu et al., 2023]. More recent research extends ASIF to include electricity generation and modal shift explicitly, leading to variants such as A-S-I-F-E that can be applied to decarbonization pathways in public transport [Casquet et al., 2025; Shammas[17]]. These applications demonstrate that ASIF provides a transparent and flexible structure for tracking transport emissions under different policy scenarios. Yet in most cases, ASIF-based emission inventories and decompositions are used ex post to evaluate policy packages or national strategies, rather than being coupled directly with heuristic network design algorithms.

Overall, the relevant literature leaves three methodological gaps for local Metro-BRT interchange design. First, many sustainability and MCDM studies evaluate pre-defined alternatives rather than testing whether a proposed transfer facility actually changes passenger paths. Second, network-design studies often combine road and transit representations in ways that can obscure the distinction between vehicular movement, walking access, transit service, and explicit intermodal transfer. Third, demand and transfer-design effects can become confounded when the OD matrix is regenerated after each network change. The present study addresses these gaps through a layered passenger graph, fixed-OD evaluation, coordinate-based transfer-candidate screening, and transparent algorithm benchmarking. This paper makes four contributions:

1. A reproducible layered passenger-network representation for Isfahan that separates walking access/egress, Metro and BRT service, and explicit intermodal transfer links from vehicular road movement.
2. A fixed-OD gravity-based evaluation procedure that separates network-design effects from endogenous regeneration of demand and treats the gravity deterrence coefficient transparently through sensitivity analysis.
3. A coordinate-based Metro-BRT candidate-generation and network-effect screening procedure, combined with an upper-bound transfer budget ($|S| <= 5$) and parsimony tie-breaking.
4. Direct benchmarking of improved ACO, standard ACO, and greedy forward selection on the corrected network, together with structural single-link, pair, and targeted triple screening.

The remainder of this paper is organized as follows. Section 2 describes the passenger-network, demand, candidate-generation, and optimization methods. Section 3 reports calibration, structural screening, and benchmark results. Section 4 summarizes conclusions, practical implications, limitations, and future research. Figure 1 summarizes the fixed-OD Metro-BRT transfer design in Isfahan.

https://doi.org/10.1038/s41598-026-74249-1

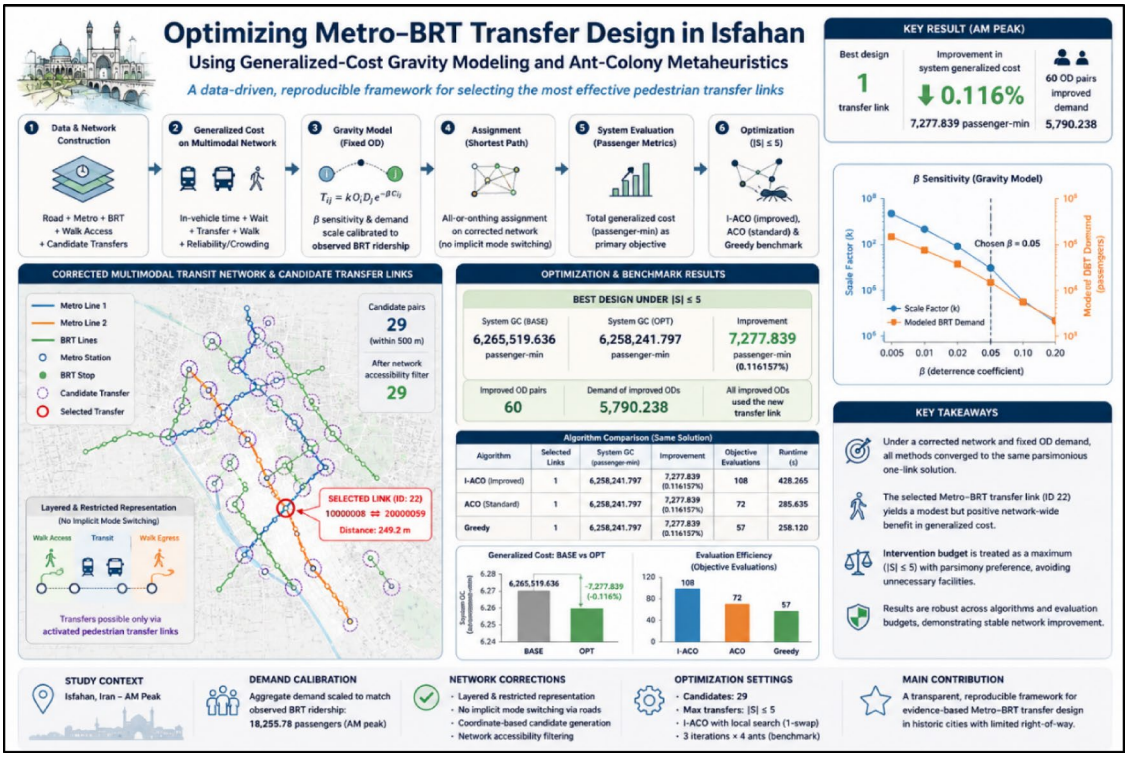


Fig. 1 Workflow for fixed-OD Metro-BRT transfer design in Isfahan.

Table 1 Parameters and modeling assumptions used in the fixed-OD transfer-design analysis.

Component	Parameter	Symbol	Value / treatment
Walking	Walking speed	v_{walk}	4.8 km/h
Metro service	Expected waiting time	$t_{wait,M}$	7.5 min (15-min headway; random arrivals)
BRT service	Expected waiting time	$t_{wait,B}$	5.0 min central parametric case
Boarding/exit	Boarding and exit penalties	π_{entry}, π_{exit}	0.5 min each
Transfer	Transfer inconvenience	$\pi_{transfer}$	2.0 min central parametric case
Reliability/crowding	Additional allowance	π_{RC}	1.0 min central parametric case
Gravity model	Deterrence coefficient	βg	0.05 central; 0.005-0.20 sensitivity
Demand	Observed BRT AM ridership	$Q_{BRT,obs}$	18,255.78 passengers
Demand	OD treatment	Tij	Fixed for BASE and OPT
Candidate generation	Maximum geographic distance	r_{max}	500 m
Optimization	Maximum number of selected links	P_{max}	5; upper-bound constraint
Optimization	Primary objective	GC(S)	Σ_i Σ_{j≠i} T^0_ij C_ij(S), passenger-min
I-ACO/ACO pilot	Ants x iterations	n_{ant} x n_{iter}	4 × 3
I-ACO	Evaporation rate	ρ	0.20
I-ACO/ACO	Pheromone / heuristic exponents	α, β_h	1.0, 2.0

Materials and methods

Study area and data basis

The study focuses on the Isfahan AM peak and on local pedestrian connections between Metro stations and BRT stops. The computational inputs comprise the directed road network, Metro service edges, BRT service edges, station and stop coordinates, walking-access connectors, zone representative nodes, and the available aggregate AM-peak BRT ridership observation. The empirical information available for the final optimization does not constitute a complete observed spatial OD matrix, AFC-derived OD table, or station-to-station passenger-flow dataset. The aggregate ridership observation is therefore used only to anchor demand magnitude; it is not presented as validation of the spatial OD pattern. This distinction is maintained throughout the revised manuscript to avoid conflating aggregate demand scaling with OD validation.

Metro stations and BRT stops are represented with distinct synthetic identifiers so that transit layers do not collapse onto shared road nodes. BRT access connectors were audited against actual BRT service nodes. Connectors requiring more than 500 m of modeled walking access were excluded from the corrected passenger graph. Transfer candidates were then regenerated from geographic Metro-station and BRT-stop coordinates using direct geographic distance and retained when the candidate distance did not exceed 500 m and both endpoints were connected to the corrected service network.

Passenger-network representation

The passenger graph is state-separated to prevent implicit mode switching through vehicular road links. A transit trip is represented by three stages: (1) pre-transit walking access on the street topology, (2) a transit-active layer containing Metro service, BRT service, and explicitly activated Metro-BRT transfer links, and (3) post-transit walking egress. Road topology is used for walking access and egress at walking speed, whereas vehicular road travel times are not available as intermediate links inside a transit path. Therefore, a passenger cannot alight from one transit mode, traverse the road network at vehicle speed, and board another mode unless an explicit transfer facility is available.

For the central generalized-cost case, walking speed is 4.8 km/h. Metro expected waiting time is 7.5 min, based on the available 15 min headway and a random-arrival assumption. BRT waiting time is set to 5.0 min in the central scenario. Boarding and exit penalties are 0.5 min each, the explicit transfer-inconvenience penalty is 2.0 min, and a 1.0 min reliability/crowding allowance is included. These quantities are modeling assumptions rather than field-calibrated distributions. They are retained to represent major components of passenger impedance, but the present data do not support claims of behavioral calibration. Fare is excluded from generalized cost because a locally validated value of time and a consistently documented Metro and BRT fare representation were unavailable. Consequently, the generalized-cost results should be interpreted as passenger-time-based screening results rather than a complete behavioral utility model.

For an OD pair (i, j), generalized cost is defined as the minimum feasible passenger-path cost on the corrected state-separated graph. The path cost includes in-vehicle service time, walking access/egress, waiting, boarding/exit overheads, explicit Metro-BRT transfer time and inconvenience, and the reliability/crowding allowance used in the stated scenario according to Eq. (1):

$$C_{ij}(S) = \min_{p \in P_{ij}(S)} [T_p^{iv} + T_p^{walk} + T_p^{wait} + T_p^{b/e} + T_p^{tr} + T_p^{rc}] \quad (1)$$

Gravity demand scaling sensitivity and fixed-od evaluation

Trip distribution is represented by a doubly constrained gravity model with exponential deterrence. Using the baseline corrected generalized-cost matrix, the fixed OD matrix is generated according to Eq. (2), where O_i and D_j denote the modeled zonal production and attraction marginals, A_i and B_j are balancing factors, and β_g is the gravity deterrence coefficient.

$$T_{ij}^0 = A_i O_i B_j D_j \exp\left[-\beta_g C_{ij}^0\right],\ i \neq j \tag{2}$$

Because the available empirical information consists of one aggregate AM-peak BRT ridership observation, the gravity deterrence coefficient and total demand scale cannot be jointly identified statistically. Accordingly, βg is not described as calibrated. It is treated as a sensitivity parameter over 0.005–0.20, with βg = 0.05 retained as the central analytical case. Conditional on each βg value, the aggregate scale factor is computed from observed and modeled AM-peak BRT ridership using Eq. (3). This procedure calibrates only the aggregate magnitude conditional on an assumed βg; it does not validate the spatial OD pattern or establish βg as a behaviorally estimated parameter.

$$k\left(\beta_g\right) = \frac{Q_{BRT}^{obs}}{Q_{BRT}^{model}\left(\beta_g\right)},\ O_i = kO_i^{ref},\ D_j = kD_j^{ref} \tag{3}$$

The resulting OD matrix is generated once and then held fixed for all baseline and intervention evaluations, as stated in Eq. (4). This fixed-OD condition isolates the network-design effect from generated-demand effects that would arise if the gravity matrix were recomputed after every candidate-set change.

$$T_{ij}^{BASE} = T_{ij}^{OPT} = T_{ij}^0 \tag{4}$$

The primary network objective is the fixed-demand passenger-weighted generalized cost as Eq. (5):

$$GC\left(S\right) = \sum\nolimits_i \sum\nolimits_{j \neq i} T_{ij}^0 C_{ij}\left(S\right) \tag{5}$$

Transfer-candidate generation and structural screening

Coordinate-based generation produced 29 Metro-BRT candidate pairs within 500 m after corrected network-access filtering. Each candidate was first evaluated individually by temporarily activating the transfer and recomputing shortest passenger paths under the fixed OD matrix. A candidate was considered individually effective only if it reduced generalized cost for at least one positive-demand OD pair. To avoid prematurely discarding links that might be useful only in combination, all 406 candidate pairs were subsequently tested, followed by targeted triple-combination screening.

Transfer-selection optimization

Let x_m indicate whether transfer candidate m is activated. The intervention budget is formulated as an upper-bound cardinality constraint rather than a compulsory five-link design as Eq. (6). The optimization is lexicographic: total generalized cost is minimized first and, among equal-cost solutions within numerical tolerance, the design with fewer activated transfer facilities is preferred in Eq. (7).

$$x_m \in \{0,1\},\ S = \{m : x_m = 1\},\ \sum\nolimits_{m=1}^{M} x_m \leq P_{max} = 5 \tag{6}$$

$$S^* = \arg \min_{S:\ |S| \leq 5} \left(GC\left(S\right), |S|\right)_{lex} \tag{7}$$

Three search strategies are evaluated on the corrected model. In ACO, an available candidate is selected probabilistically using pheromone intensity and heuristic desirability as in Eq. (8), where α controls pheromone influence and β_h controls heuristic influence. Standard ACO uses pheromone evaporation and reinforcement, whereas I-ACO employs rank-based reinforcement as Eq. (9) together with limited 1-swap local refinement. Greedy forward selection provides a deterministic benchmark and stops when no further positive marginal generalized-cost gain is found.

$$\rho_m = \frac{\tau_m^{\alpha} \eta_m^{\beta_h}}{\sum_{k \in A} \tau_k^{\alpha} \eta_k^{\beta_h}}, \; m \in A \tag{8}$$

$$\tau_m^{(t+1)} = (1-\rho)\tau_m^{(t)} + \sum_{r=1}^{R} (R-r+1) \frac{GC_{BASE}}{GC\left(S_r^{(t)}\right)} 1\left(m ? S_r^{(t)}\right) + 2 \frac{GC_{BASE}}{GC\left(S_{best}^{(t)}\right)} 1\left(m ? S_{best}^{(t)}\right) \tag{9}$$

Notation note: β_g denotes the gravity-model deterrence coefficient, whereas β_h denotes the ACO heuristic exponent; the two parameters are unrelated. The corrected benchmark is used to establish network consistency and cross-method agreement.

Results

Figure 2 presents the edge composition of the corrected multimodal passenger-network inputs used in the Isfahan AM-peak analysis. The baseline network contains 2,318 input edges, of which road links constitute the dominant share, with 2,008 edges (86.63%). BRT service is represented by 154 edges (6.64%), while repaired BRT pedestrian-access connectors contribute 122 edges (5.26%). Metro access and Metro service account for 18 edges (0.78%) and 16 edges (0.69%), respectively. Taken together, BRT service and BRT-access edges represent 11.90% of the corrected network inputs, whereas Metro service and access account for 1.47%. This distribution reflects the road-dominant structure of the urban network while preserving explicit public-transport and pedestrian-access components required for multimodal routing. Importantly, candidate Metro–BRT transfer links are not counted as active baseline edges. After coordinate-based screening and network-accessibility filtering, 29 feasible candidate transfer pairs within 500 m were retained for optimization, while the baseline scenario contains no newly activated Metro–BRT transfer. In the optimized scenario, only one logical Metro–BRT transfer

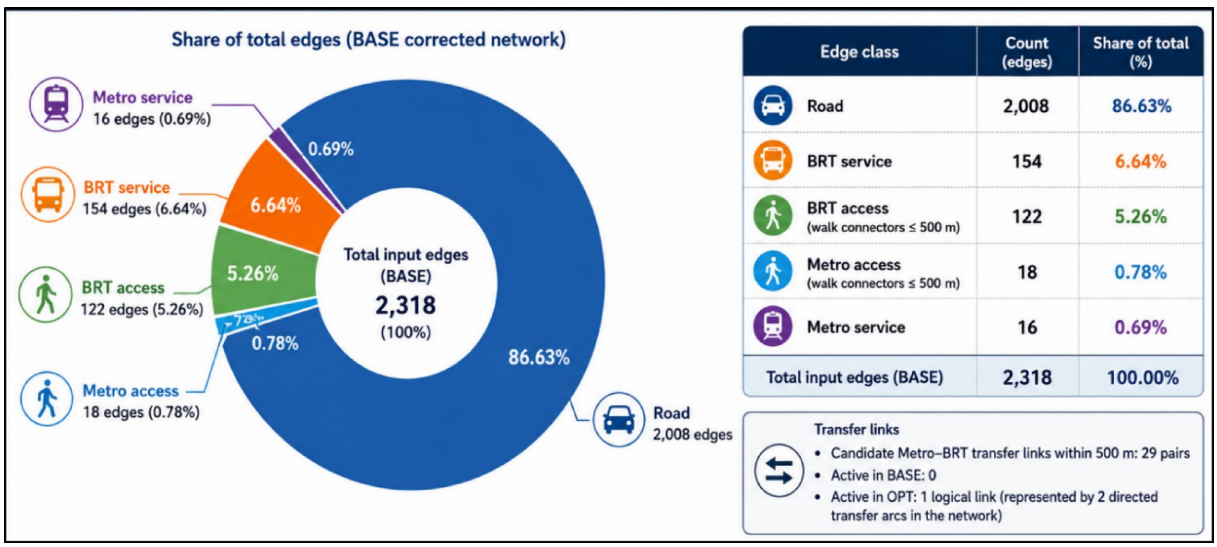


Fig. 2 Edge composition of the multimodal passenger-network inputs for the Isfahan AM-peak analysis.

link is activated; because the network is directed, this logical connection is represented by two directed transfer arcs. This distinction between candidate, baseline-active, and optimized-active links is essential for avoiding the ambiguity present in the earlier network representation. The corrected topology therefore ensures that intermodal switching can occur only through explicitly modeled pedestrian transfer links rather than implicitly through shared road nodes, providing a structurally consistent basis for the fixed-OD generalized-cost evaluation and subsequent optimization.

Figure 3 compares the system-wide passenger generalized cost under the baseline and optimized transfer configurations while holding the OD matrix fixed. The baseline generalized cost is 6,265,519.636 passenger-min, whereas activation of the optimized Metro–BRT transfer reduces this value to 6,258,241.797 passenger-min. The resulting reduction is 7,277.839 passenger-min, equivalent to 0.116157% of the baseline generalized cost. Because the same fixed OD matrix is assigned in both scenarios, this difference represents the effect of the network intervention itself rather than a change caused by regeneration of travel demand. The optimized design consists of a single logical transfer connection, candidate 22, linking nodes 10,000,008 and 20,000,059 over an approximately 249.2-m pedestrian connection. This intervention improves the generalized costs of 60 positive-demand OD pairs representing 5,790.238 demand units, and all affected OD paths use the newly activated transfer connection. Although the aggregate percentage reduction is modest, the result demonstrates a spatially concentrated and behaviorally interpretable benefit under the corrected restricted-transit representation.

To evaluate whether the corrected optimum depended on the search procedure, I-ACO was benchmarked against standard ACO and greedy forward selection using the same fixed-OD network representation and transfer-candidate set.

Figure 4 compares the computational effort and solution consistency of the improved Ant Colony Optimization (I-ACO), standard ACO, and deterministic greedy benchmark under the corrected fixed-OD formulation. All three methods converged to the same parsimonious one-link design, selecting candidate 22, which connects Metro node 10,000,008 to BRT node 20,000,059 through a 249.2-m pedestrian transfer. The selected intervention produces an identical reduction in total system generalized cost for all three methods, equal to 7,277.839 passenger-min, corresponding to a 0.116157% improvement relative to the corrected baseline. This agreement confirms that the selected transfer is not an artifact of a particular search procedure and that the optimum is structurally well defined under the present candidate set and generalized-cost representation. The methods differ, however,

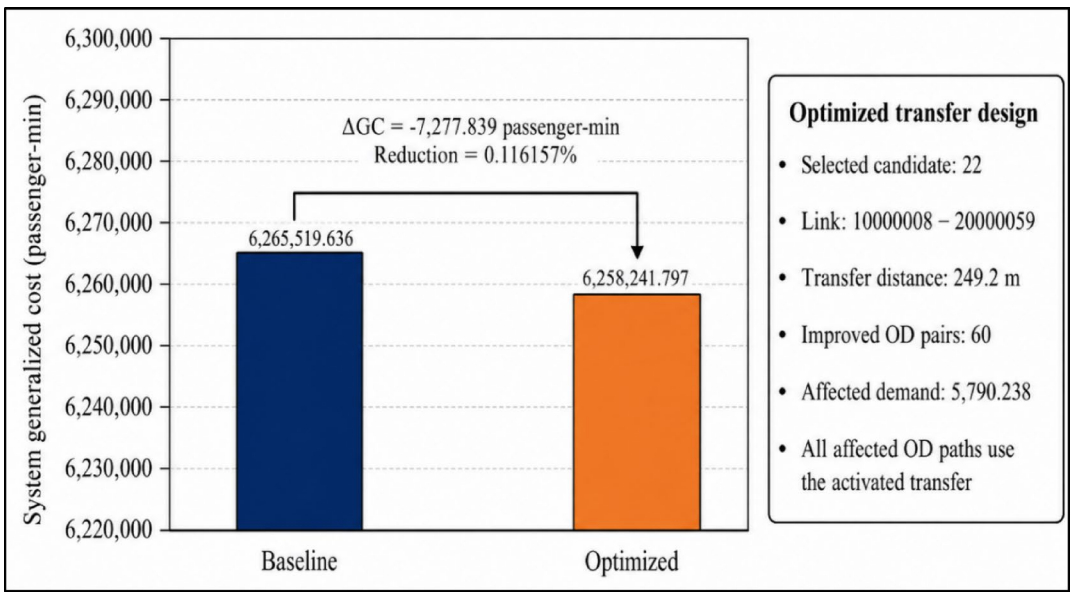


Fig. 3 Comparison of fixed-OD system generalized cost between the baseline and optimized Metro–BRT transfer configurations.

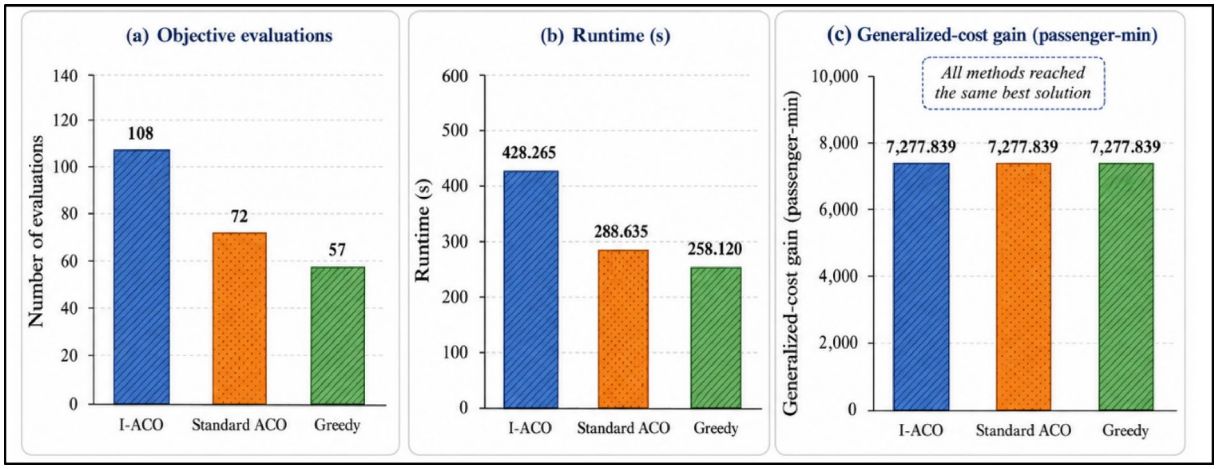


Fig. 4 Algorithm benchmark under the fixed-OD formulation.

Table 2 Network-effect screening of the individually effective Metro–BRT transfer candidates.

Candidate	Metro node	BRT node	Distance (m)	Improved OD pairs	Affected demand	GC improvement (passenger-min)
21	10,000,008	20,000,058	379.8	60	5,790.238	3,040.612
22	10,000,008	20,000,059	249.2	60	5,790.238	7,277.839

in computational effort. I-ACO required 108 objective-function evaluations and approximately 428.265 s of runtime, standard ACO required 72 evaluations and approximately 285.635 s, while the greedy method reached the same solution using only 57 evaluations and approximately 258.120 s. Therefore, in the present corrected case, the enhanced I-ACO did not provide a better objective value than the simpler benchmark methods; instead, its main contribution is demonstrating that the proposed search framework is capable of recovering the same stable solution under a stochastic metaheuristic formulation. The greedy method was computationally the most efficient among the tested approaches, whereas I-ACO incurred the highest computational cost because of its rank-based pheromone reinforcement and local-refinement operations. The common solution improves 60 positive-demand OD pairs representing 5,790.238 demand units, and all affected OD paths use the newly activated Metro–BRT transfer. These results indicate that the benefit of the intervention is concentrated spatially and behaviorally rather than distributed uniformly across the entire network. Consequently, the revised interpretation emphasizes cross-method solution consistency and parsimony rather than claiming numerical superiority of I-ACO. This distinction is important because it provides a more conservative and reproducible assessment of the optimization framework while directly addressing concerns regarding benchmark comparison and computational transparency.

To identify which geometrically feasible transfer connections produce an actual network benefit, all 29 candidates were first evaluated individually under the corrected fixed-OD model.

Twenty-nine feasible coordinate-based candidates were screened under the corrected central fixed-OD model. Only candidates 21 and 22 produced a positive individual generalized-cost improvement; candidate 22 was the best-performing single-link alternative.

Table 2 summarizes the network-effect screening of the individually effective Metro–BRT transfer candidates under the corrected fixed-OD formulation. Among the 29 feasible coordinate-based candidate pairs retained after spatial and network-accessibility filtering, only candidates 21 and 22 produced a positive individual reduction in system generalized cost. Both candidates affect the same 60 positive-demand OD pairs, representing 5,790.238 demand units; however, candidate 22 provides a substantially larger generalized-cost benefit. Specifically, candidate 21 yields a reduction of 3,040.612 passenger-min, whereas candidate 22 reduces system generalized cost by 7,277.839 passenger-min. Candidate 22 also has the shorter pedestrian connection, approximately 249.2 m

compared with 379.8 m for candidate 21. These results indicate that the useful transfer opportunity is highly spatially concentrated and provide a transparent basis for selecting candidate 22 as the best single-link intervention.

Figure 5 illustrates the best-so-far convergence behavior of I-ACO and standard ACO under the fixed-OD formulation. Both stochastic algorithms identified the same one-link solution from the first iteration and retained the same best generalized-cost value over the subsequent iterations.

The baseline system generalized cost was 6,265,519.636 passenger-min, whereas both algorithms reached a best value of 6,258,241.797 passenger-min, corresponding to a reduction of 7,277.839 passenger-min (0.116157%). The common solution was candidate 22, connecting Metro node 10,000,008 to BRT node 20,000,059 through a 249.2-m pedestrian transfer.

The overlap of the two best-so-far trajectories shows that, within this restricted fast benchmark, both stochastic procedures recovered the same best solution. No additional improvement was observed after iteration 1. This is consistent with the deterministic greedy benchmark, which also selected candidate 22. This agreement is a computational consistency check only; it is not evidence of behavioral validity, statistical robustness, or superiority of I-ACO. The principal difference among the tested methods in this experiment is computational effort.

The experiment shown in Fig. 5 is a computationally restricted fast benchmark with three iterations and is intended to demonstrate solution consistency and convergence behavior after correction of the network and demand formulations. It is not presented as a substitute for a full 20–30-run statistical robustness analysis. Accordingly, the revised manuscript does not claim statistically superior convergence of I-ACO; instead, Fig. 5 provides evidence that both stochastic search procedures recover the same parsimonious optimum rapidly under the corrected fixed-OD representation.

Figure 6 Robustness and internal-consistency checks supporting the corrected fixed-OD Metro–BRT transfer-design results. The panels summarize (**a**) sensitivity treatment of the gravity deterrence coefficient, (**b**) coordinate- and network-based candidate screening, (**c**) exhaustive pair and targeted triple combination tests, (**d**) fixed-OD consistency between BASE and OPT, and (**e**) agreement among I-ACO, standard ACO, and greedy search.

Panel (a) summarizes the sensitivity treatment of the gravity deterrence coefficient, βg. Because only one aggregate observed AM-peak BRT ridership count was available, βg could not be jointly identified with the overall demand scale. Accordingly, βg was treated as a sensitivity parameter rather than as a statistically calibrated coefficient. Values from 0.005 to 0.20 were examined, and $\beta g = 0.05$ was retained as the central case. For each assumed βg, the aggregate demand scale required to reproduce the observed AM-peak BRT ridership was evaluated. This analysis characterizes sensitivity of demand scaling and mean generalized cost; it does not demonstrate

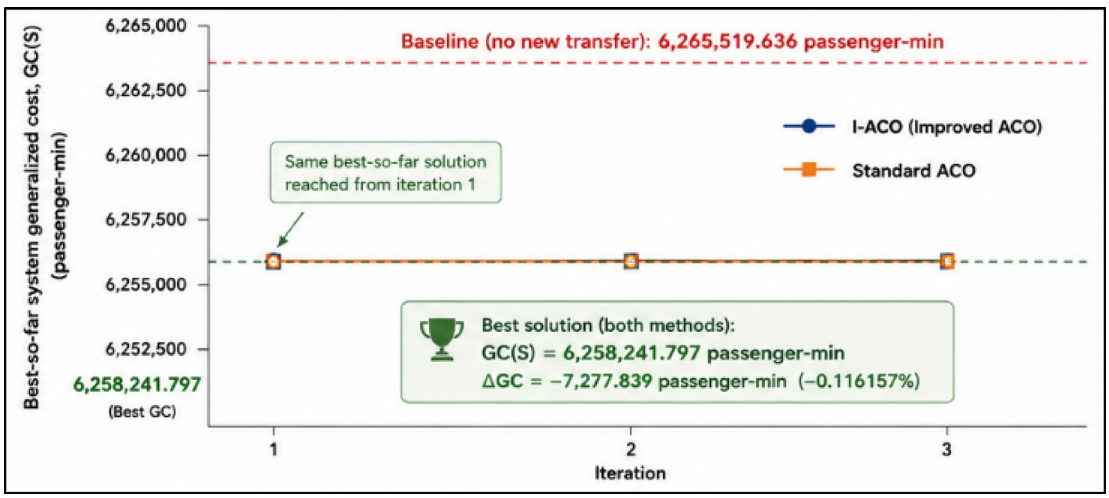


Fig. 5 Convergence behavior of ACO and I-ACO in the fixed-OD benchmark.

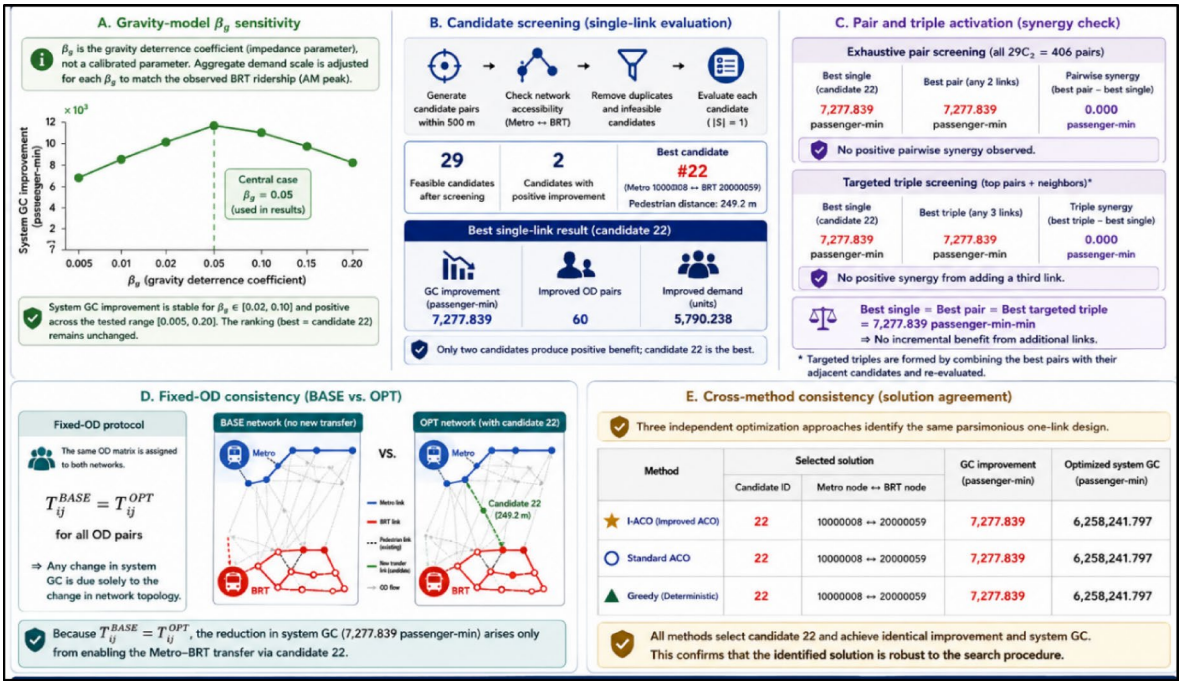


Fig. 6 summarizes the principal robustness and internal-consistency checks introduced after revision of the demand, network, and optimization formulations.

that candidate 22 is invariant across the full βg range. The latter remains an unresolved robustness question and is stated explicitly as a limitation.

Panel (b) presents the corrected transfer-candidate screening procedure. Metro-station and BRT-stop coordinates were used to construct candidate pedestrian connections, followed by the 500-m distance criterion and corrected network-accessibility filtering. This procedure retained 29 feasible Metro–BRT candidate pairs. Each candidate was then evaluated individually under the same fixed-OD and restricted-transit representation. Only two candidates produced a positive reduction in system generalized cost, and candidate 22 provided the largest benefit. Candidate 22 connects Metro node 10,000,008 to BRT node 20,000,059 through an approximately 249.2-m pedestrian transfer and reduces total system generalized cost by 7,277.839 passenger-min. The intervention improves 60 positive-demand OD pairs representing 5,790.238 demand units.

Panel (c) examines whether simultaneous activation of additional transfer links produces benefits beyond those obtained from the best single candidate. All (229)=406 candidate pairs were evaluated exhaustively. No positive pairwise synergy was identified: the best pair achieved the same generalized-cost reduction as candidate 22 alone, namely 7,277.839 passenger-min. A subsequent targeted triple screening, which explicitly retained the individually effective candidates in the shortlist, likewise produced no additional improvement. Hence, within the exhaustive pair and targeted triple tests, the best single-link, best pair, and best tested triple all attained the same objective value. This finding provides the empirical rationale for replacing the former compulsory cardinality constraint with the upper-bound formulation $|S| \leq 5$ and for applying a parsimony rule that favors the smallest design among solutions with equivalent generalized cost.

Panel (d) verifies the fixed-OD protocol that is central to the corrected before–after comparison. The same OD matrix is assigned to both network configurations, such that $T_{ijBASE} = T_{ijOPT}$ for every OD pair. The baseline contains no newly activated Metro–BRT intervention transfer, whereas the optimized network differs only through activation of candidate 22. Consequently, the observed reduction in system generalized cost cannot be attributed to regeneration of travel demand after the network is modified; it represents the modeled effect of the

network-topology intervention under an identical demand matrix. This directly addresses the potential generated-demand confounding present in the earlier formulation.

Panel (e) provides an independent cross-method consistency check. I-ACO, standard ACO, and deterministic greedy forward selection all identified the same parsimonious one-link design, candidate 22, and all produced the same optimized system generalized cost of 6,258,241.797 passenger-min. Relative to the corrected baseline value of 6,265,519.636 passenger-min, this corresponds to an improvement of 7,277.839 passenger-min, or 0.116157%. The agreement among methods indicates that the selected solution is not dependent on a particular search mechanism in the present corrected problem. However, this cross-method agreement is interpreted as evidence of structural solution consistency rather than as a substitute for a full multi-run statistical comparison of the stochastic algorithms.

Taken together, the checks summarized in Fig. 6 show that the corrected result is supported by transparent demand-parameter treatment, explicit candidate screening, absence of additional benefit from the tested multi-link combinations, strict fixed-OD comparison, and agreement among three independent search procedures. The resulting recommendation is therefore a parsimonious one-link intervention rather than the compulsory five-link configuration reported in the earlier formulation. At the same time, the relatively small aggregate improvement of 0.116157% is interpreted conservatively as a localized modeled network benefit rather than evidence of a large system-wide effect.

To determine whether the identified optimum depended on the search strategy, the corrected problem was evaluated using I-ACO, standard ACO, and greedy forward selection.

All three methods identified the same parsimonious one-link solution. The corrected baseline generalized cost was 6,265,519.636 passenger-min. The stochastic results shown here are from the fast benchmark and are not presented as a substitute for a full 20–30-run statistical robustness study.

Table 3 compares I-ACO, standard ACO, and deterministic greedy forward selection under the corrected fixed-OD formulation. All three methods identified the same parsimonious one-link design, candidate 22, and produced the same optimized system generalized cost of 6,258,241.797 passenger-min. Relative to the corrected baseline generalized cost of 6,265,519.636 passenger-min, the common solution yields a reduction of 7,277.839 passenger-min, corresponding to 0.116157%. The algorithms therefore do not differ in solution quality in the present corrected case; instead, their main differences concern computational effort. I-ACO required 108 objective-function evaluations and 428.265 s, standard ACO required 72 evaluations and 285.635 s, and greedy search required 57 evaluations and 258.120 s. Accordingly, the revised interpretation emphasizes cross-method solution consistency rather than superiority of I-ACO. The agreement among three distinct search procedures provides additional evidence that candidate 22 is a stable optimum within the corrected candidate set and objective formulation.

After identifying the most effective individual transfer, combination tests were performed to determine whether multi-link designs create complementary or synergistic benefits.

Pair screening was exhaustive over all 406 candidate pairs. Triple screening was targeted rather than exhaustive; therefore, the manuscript should state ‘no synergy was found in exhaustive pair screening or targeted triple screening’ rather than claiming exhaustive verification of all triples.

Table 4 evaluates whether activating additional transfer facilities provides incremental benefit beyond the best single-link design. Individual screening identified candidate 22 as the best single connection with a generalized-cost reduction of 7,277.839 passenger-min. All 406 candidate pairs were then evaluated exhaustively. A subsequent targeted screening of 100 three-link combinations likewise produced the same best generalized-cost

Table 3 Comparison of optimization methods under the corrected fixed-OD formulation.

Method	Selected candidate	No. links	Optimized GC (passenger-min)	GC gain (passenger-min)	Gain (%)	Objective evaluations	Run-time (s)
I-ACO	22	1	6,258,241.797	7,277.839	0.116157	108	428.265
Standard ACO	22	1	6,258,241.797	7,277.839	0.116157	72	285.635
Greedy	22	1	6,258,241.797	7,277.839	0.116157	57	258.120

Table 4 Marginal benefit and synergy tests for multi-link transfer designs.

Design test	Combinations evaluated	Best GC gain (passenger-min)	Increment over best single (passenger-min)	Interpretation
Single link	29	7,277.839	—	Best single: candidate 22
All pairs	406	7,277.839	0.000	No positive pairwise synergy
Targeted triples	100	7,277.839	0.000	No incremental benefit in tested triples

Table 5 Sensitivity of the gravity-model demand scaling to the deterrence coefficient βg.

β_g	Modeled BRT demand before scaling	BRT share (%)	Scale factor	Scaled total demand	Mean generalized cost (min)
0.005	18,765.801	19.447	0.972822	97,282.179	10.785
0.010	18,672.091	19.387	0.977704	97,770.412	10.673
0.020	18,478.133	19.266	0.987967	98,796.671	10.436
0.030	18,274.844	19.143	0.998957	99,895.682	10.182
0.050	17,836.916	18.890	1.023483	102,348.300	9.640
0.075	17,223.372	18.542	1.059942	105,994.230	8.934
0.100	16,534.325	18.139	1.104114	110,411.399	8.252
0.150	14,983.564	17.153	1.218387	121,838.702	7.090
0.200	13,341.145	16.003	1.368382	136,838.183	6.223

reduction of 7,277.839 passenger-min, with no incremental improvement over the best single-link design. These results demonstrate that, within the exhaustive pair and targeted triple experiments, additional transfer links do not improve the objective once candidate 22 is activated. This finding directly supports the revised constraint $|S| \leq 5$ and the lexicographic parsimony rule, under which the smallest design is preferred when multiple solutions have equivalent generalized cost.

Because the available ridership observation is insufficient to identify both impedance sensitivity and total demand magnitude, a conditional scaling analysis was performed over a range of plausible βg values.

βg is treated as a sensitivity parameter rather than as a statistically calibrated coefficient. For each assumed βg, the aggregate demand scale was adjusted conditionally to reproduce the observed AM-peak BRT ridership of 18,255.78 passengers. The central case used in the corrected fixed-OD analysis is $\beta g = 0.05$.

Table 5 reports the sensitivity of the gravity-model demand scaling to the deterrence coefficient βg. Because the available empirical demand information consists of one aggregate observed AM-peak BRT ridership value, βg and total demand scale cannot be jointly estimated from the available data. The deterrence coefficient was therefore treated as a sensitivity parameter rather than as a statistically calibrated behavioral coefficient. Values between 0.005 and 0.20 were examined. As βg increases, modeled BRT demand before scaling decreases from 18,765.801 to 13,341.145 trips and the implied BRT share decreases from 19.447% to 16.003%. Consequently, a progressively larger aggregate scale factor is required to reproduce the observed AM-peak BRT ridership, increasing from 0.972822 at $\beta g = 0.005$ to 1.368382 at $\beta g = 0.20$. The central case $\beta g = 0.05$ corresponds to a scale factor of 1.023483 and was adopted for construction of the fixed OD matrix used in the corrected optimization experiments. This sensitivity analysis makes explicit that the available observation is used to anchor aggregate demand magnitude, while βg remains a modeling assumption subject to sensitivity analysis.

Figure 7 integrates the corrected candidate-screening, spatial interpretation, multi-link comparison, and algorithm-benchmark results for the fixed-OD restricted-transit formulation.

Panel (a) summarizes the transfer-screening process. Starting from 29 coordinate-derived Metro–BRT candidate pairs that satisfied the 500-m proximity and network-accessibility requirements, only two candidates produced a positive individual reduction in system generalized cost. Among these, candidate 22 was identified as

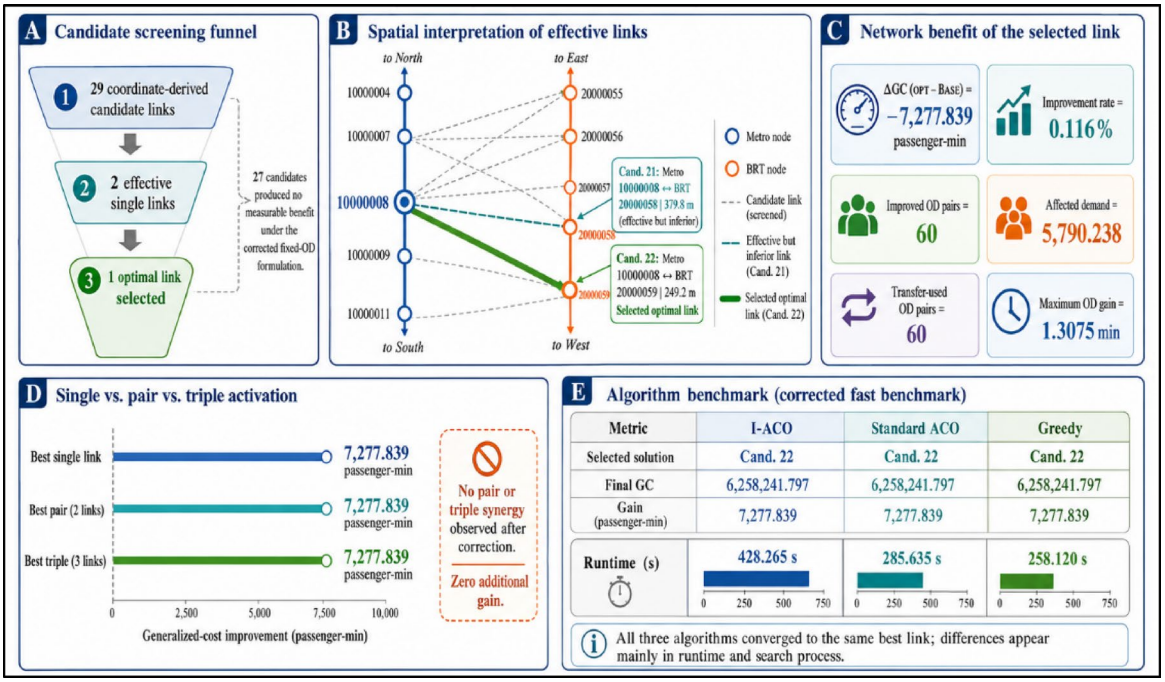


Fig. 7 Corrected transfer-screening and optimization results under the fixed-OD restricted-transit formulation.

the best-performing transfer and was retained as the parsimonious optimal design. The remaining 27 candidates produced no measurable generalized-cost improvement under the corrected central fixed-OD formulation.

Panel (b) provides a spatial interpretation of the effective transfer alternatives. Both effective candidates connect Metro node 10,000,008 to nearby BRT nodes, indicating that the useful transfer opportunity is spatially concentrated around this part of the multimodal corridor. Candidate 21 connects Metro node 10,000,008 to BRT node 20,000,058 over approximately 379.8 m, whereas candidate 22 connects the same Metro node to BRT node 20,000,059 over a shorter pedestrian distance of approximately 249.2 m. Candidate 22 produces the greater network benefit and is therefore selected as the final intervention. This spatial representation also confirms that the optimized transfer is a local pedestrian connection rather than an unrealistic long-range network shortcut.

Panel (c) quantifies the network effect of the selected transfer. Activation of candidate 22 reduces total system generalized cost by 7,277.839 passenger-min, equivalent to a 0.116157% reduction relative to the corrected baseline. The intervention improves 60 positive-demand OD pairs representing 5,790.238 demand units, and all 60 affected OD paths use the newly activated Metro–BRT connection. The maximum improvement observed for an individual OD pair is approximately 1.3075 min. These results show that the aggregate system benefit is modest but behaviorally interpretable and concentrated among OD movements for which the new transfer creates a competitive multimodal route.

Panel (d) examines whether selecting more than one transfer link yields additional generalized-cost benefit. The best single-link design, the best pair among all $(229)=406$ combinations, and the best targeted triple design all achieve the same generalized-cost reduction of 7,277.839 passenger-min. Thus, exhaustive pair screening identified no positive pairwise synergy, and the targeted triple screening likewise found no incremental benefit from adding a third transfer. This result provides direct empirical support for treating the intervention budget as an upper bound, $|S|\leq 5$, rather than forcing exactly five transfer links. Under the adopted parsimony rule, candidate 22 alone is preferred because additional links do not improve the objective.

Panel (e) compares the corrected solution obtained using I-ACO, standard ACO, and deterministic greedy forward selection. All three methods independently identify candidate 22 and produce the same optimized generalized cost of 6,258,241.797 passenger-min and the same generalized-cost improvement of 7,277.839 passenger-min.

The methods differ mainly in computational effort: I-ACO required 428.265 s, standard ACO required 285.635 s, and greedy required 258.120 s in the fast benchmark. Accordingly, the revised interpretation does not claim numerical superiority of I-ACO; instead, the agreement among three distinct search procedures is used as evidence that the identified one-link solution is structurally stable within the corrected problem formulation.

Overall, Fig. 7 shows that the corrected optimization problem is characterized by a highly concentrated transfer benefit: only two of the 29 feasible candidates are individually effective, candidate 22 dominates the available alternatives, and adding further transfer links does not produce additional generalized-cost improvement within the exhaustive pair and targeted triple tests. The resulting recommendation is therefore a single, spatially plausible Metro–BRT pedestrian transfer rather than the compulsory five-link configuration used in the earlier formulation.

Discussion

The corrected analysis provides a substantially different interpretation of Metro–BRT transfer design than the earlier formulation. Under the fixed-OD and restricted-transit representation, the network-wide benefit of transfer intervention is highly concentrated rather than broadly distributed across many candidate connections. Of the 29 feasible coordinate-based candidates, only two produced a positive individual reduction in generalized cost, and candidate 22 clearly dominated candidate 21. The selected link connects Metro node 10,000,008 to BRT node 20,000,059 through an approximately 249.2-m pedestrian transfer and reduces total system generalized cost by 7,277.839 passenger-min, equivalent to 0.116157% of the corrected baseline. Although this percentage is modest at the system level, the intervention improves 60 positive-demand OD pairs representing 5,790.238 demand units, indicating a localized but behaviorally interpretable benefit.

A key methodological implication is that the benefit of the selected transfer emerges only after eliminating implicit mode switching through shared road and transit nodes. In the corrected restricted-transit representation, passenger movement between Metro and BRT services can occur only through explicitly activated pedestrian transfer links. This change is important because it isolates the actual contribution of transfer infrastructure from artificial path-shortening effects that can arise in an insufficiently layered multimodal graph. The revised network therefore provides a more defensible representation of interchange behavior and ensures that the observed improvement can be attributed to the newly activated transfer itself.

The fixed-OD formulation also changes the interpretation of the reported performance gains. In the earlier approach, the OD matrix was recomputed after each network modification, making it difficult to distinguish true network-design benefits from changes induced by demand regeneration. In the revised framework, the same OD matrix is assigned to both the baseline and optimized networks. Consequently, $T_{ijBASE}=T_{ijOPT}$,

and the difference in system generalized cost reflects only the change in network topology. This correction directly strengthens the causal interpretation of the before–after comparison and removes an important source of confounding.

The candidate-combination analysis further supports a parsimonious interpretation of the optimal design. Candidate 22 alone yields a generalized-cost reduction of 7,277.839 passenger-min. Exhaustive evaluation of all 406 candidate pairs produced no additional improvement beyond this value, and the targeted triple screening likewise identified no incremental benefit. Thus, within the exhaustive pair and targeted triple analyses, the best single-link, best pair, and best tested triple all achieve the same objective value. This result justifies replacing the former compulsory five-link requirement with the upper-bound constraint $|S|\leq 5$, combined with a lexicographic parsimony rule that favors the smallest design among solutions with equivalent generalized cost. Forcing five transfer links would otherwise introduce facilities with no measurable marginal benefit under the corrected central model.

The algorithm benchmark provides a second important interpretation. I-ACO, standard ACO, and deterministic greedy forward selection all identified the same one-link solution and the same optimized generalized cost. The methods therefore differ primarily in computational effort rather than solution quality. I-ACO required 108

objective evaluations and 428.265 s, standard ACO required 72 evaluations and 285.635 s, and greedy required 57 evaluations and 258.120 s in the fast benchmark. These results do not support a claim that I-ACO achieves a superior objective value in the corrected Isfahan case. Instead, the agreement among three distinct search strategies indicates that the selected solution is structurally well defined within the present candidate set and generalized-cost representation.

This finding is particularly relevant to the interpretation of metaheuristic optimization in transport-network design. A more sophisticated search method is not necessarily expected to outperform simpler methods when the corrected objective landscape contains one clearly dominant intervention and little higher-order interaction among candidates. In such cases, the value of the metaheuristic framework lies in its ability to explore the combinatorial design space systematically and confirm the stability of the identified solution rather than in producing a lower objective than every benchmark. The revised manuscript therefore emphasizes reproducibility, cross-method agreement, and transparent computational comparison rather than algorithmic superiority.

The gravity-model sensitivity analysis warrants particularly cautious interpretation. The available empirical demand information consists of one aggregate AM-peak BRT ridership observation, which is insufficient to jointly identify the deterrence coefficient and total demand scale or to validate the spatial OD pattern. Accordingly, βg is treated as a sensitivity parameter rather than as an empirically estimated behavioral coefficient. The central value $\beta g = 0.05$ is retained for the corrected fixed-OD experiments, while values from 0.005 to 0.20 characterize the sensitivity of modeled BRT demand, BRT share, demand scaling, and mean generalized cost. The present experiments do not establish that candidate 22 remains optimal for every βg value; therefore, robustness of the selected location to alternative spatial demand patterns remains a limitation rather than a demonstrated result.

From a planning perspective, the results suggest that transfer-design benefits in the studied corridor are spatially selective. The dominant candidate is not simply the shortest geometrically feasible connection; rather, its value arises from how the connection interacts with the existing Metro and BRT network structure and the distribution of OD demand. Candidate 22 is shorter than candidate 21 and produces more than twice its generalized-cost benefit, indicating that geometric proximity alone is not sufficient for prioritizing intermodal facilities. Network-effect screening is therefore essential before recommending a transfer location.

The magnitude of the corrected system-wide improvement should also be interpreted cautiously. A reduction of 0.116157% is considerably smaller than the improvements reported in the earlier formulation and should not be described as a major network-wide transformation. Instead, the result represents a modest aggregate benefit concentrated among a specific subset of OD movements. This more conservative interpretation is important because it distinguishes modeled network efficiency from claims of large operational, environmental, or behavioral impact that would require richer observed data and additional validation.

The corrected findings also change the interpretation of environmental performance. Owais[18] emphasizes that credible emission-reduction accounting for mass rapid transit requires an explicit project boundary and consistent estimation of baseline emissions, project emissions, and leakage, supported by defensible activity, occupancy, energy or fuel, and emission-factor data. The present dataset does not provide a sufficiently documented basis for that accounting chain. Therefore, CO2, NOx, PM2.5, and fuel indicators are not used as optimization objectives and no quantitative environmental-reduction claim is made. Sustainability remains part of the planning motivation, but environmental benefits would require a separate, locally calibrated assessment before they could be attributed to the proposed transfer intervention.

In relation to previous Metro–BRT and integrated-transit studies, the present analysis is best viewed as a transfer-facility selection framework rather than a full transit-network redesign model. The decision variable concerns the activation of local pedestrian interchange opportunities between existing Metro and BRT services, while routes, frequencies, and service capacities remain largely exogenous. This distinguishes the study from transit-network design problems that optimize route structures, frequencies, timetables, or system-wide transfer minimization. The methodological contribution therefore lies in combining corrected multimodal network representation, fixed-OD generalized-cost evaluation, explicit transfer screening, and combinatorial optimization within a reproducible workflow.

Two studies specifically highlighted during peer review help position the present contribution. Owais et al.[19] integrated existing bus and metro systems in Greater Cairo and designed an underground line with passenger transfers and network connectivity as central criteria, whereas Owais et al.[19] subsequently examined multiple subway lines for minimizing passenger transfers in a large urban transit network. Those studies address strategic line design and system connectivity. By contrast, the present work keeps existing Metro and BRT routes fixed and asks a narrower question: which local pedestrian interchange opportunities between existing services measurably reduce passenger generalized cost? The comparison clarifies that the current method is a transfer-facility screening and selection framework, not a substitute for full transit-line design.

Overall, the revised results indicate that the main contribution of the study is not the magnitude of the numerical improvement but the methodological transparency of the corrected evaluation. By separating demand estimation from network comparison, preventing implicit intermodal switching, screening candidate links for actual network effect, applying a parsimonious upper-bound design constraint, and comparing multiple search strategies, the revised framework provides a more defensible basis for evaluating Metro–BRT interchange interventions. These corrections lead to a smaller but more credible result and provide a clearer foundation for future extensions using observed OD data, richer behavioral assignment models, and multi-period operational data.

Limitations and future research

The revised framework provides a more defensible assessment of Metro–BRT transfer design, but several limitations should be acknowledged. The most important limitation concerns demand data. A complete observed OD matrix, AFC records, passenger surveys, and station-level boarding–alighting counts were not available for the study period. Consequently, the OD matrix was generated from the gravity-model framework rather than directly estimated from observed trip records. The available AM-peak BRT ridership observation was therefore used only to anchor the aggregate demand scale, not to claim full OD validation.

A related limitation concerns the gravity deterrence coefficient, βg. Because the available empirical information is insufficient to jointly estimate βg and the overall demand magnitude, βg was treated as a sensitivity parameter rather than as a statistically calibrated behavioral coefficient. The central value $\beta g = 0.05$ was adopted for the corrected fixed-OD experiments, while values from 0.005 to 0.20 were examined in sensitivity analysis. Future studies should estimate impedance parameters using observed OD matrices, AFC transactions, smart-card data, or stated/revealed-preference surveys.

The passenger-assignment representation is another substantive limitation. The corrected topology prevents implicit intermodal switching and restricts Metro and BRT transfers to explicitly activated pedestrian links, but route choice is still represented through a generalized-cost shortest-path/all-or-nothing assignment. This does not represent stochastic route choice, passenger heterogeneity, capacity constraints, denied boarding, within-peak dynamics, or learning. As emphasized by Owais[18], multimodal travel-demand forecasting can be strengthened by integrating data-driven or machine-learning methods with transport simulation. Future work should therefore couple richer observed demand with stochastic or schedule-based transit assignment and, where data permit, microsimulation or agent-based simulation. The present network correction resolves a topological inconsistency; it does not resolve these behavioral limitations.

Several service-quality components are represented parametrically rather than through directly observed operational distributions. In particular, BRT waiting time, transfer penalties, reliability/crowding components, and related service attributes are modeled through fixed assumptions in the generalized-cost formulation. Although these parameters allow the analysis to represent key components of passenger impedance, they do not substitute for field observations of headways, crowding, missed-boardings, transfer walking conditions, or reliability. Future studies should calibrate these components from automatic vehicle-location data, station observations, passenger surveys, and operational records.

Fare was not included in the primary generalized-cost objective because a locally defensible value of time and a fully documented fare structure for consistent Metro–BRT comparison were not available for the corrected model. Including monetary cost without a validated conversion between monetary and temporal components could introduce an additional source of uncertainty. A future extension should incorporate fare integration explicitly once value-of-time estimates and mode-specific fare information are available.

The environmental component also remains outside the primary revised objective. Earlier versions of the analysis included fuel-consumption and emission-related quantities, but the provenance, units, vehicle-flow conversion, and applicability of the available link-level attributes could not be verified with sufficient confidence. For this reason, the revised interpretation does not make strong physical claims regarding fuel or emission reductions. Future research should integrate locally validated fleet composition, speed-dependent emission factors, vehicle occupancy, and vehicle-flow estimates before environmental impacts are quantified.

The optimization analysis is also subject to computational and uncertainty limitations. The corrected fast benchmark shows that I-ACO, standard ACO, and greedy search identify the same one-link solution under the central input set, but the stochastic algorithms were not subjected to a full 20–30 independent-run statistical comparison under the final formulation. More importantly, the reported 0.116157% system-wide improvement is small relative to plausible uncertainty in demand, waiting time, transfer impedance, reliability, and other model inputs. The current evidence is therefore insufficient to claim that the magnitude of the benefit is statistically distinguishable from input uncertainty. No undocumented binary-logit or probabilistic sensitivity experiment is claimed in this revision. Future work should propagate uncertainty jointly across demand and service parameters, report confidence intervals for network benefits, and test whether the selected candidate remains optimal across those scenarios.

The candidate-combination analysis should likewise be interpreted within its exact scope. All 406 candidate pairs were evaluated exhaustively, whereas the triple analysis was targeted rather than exhaustive. Accordingly, the absence of additional benefit is fully established for all pairs and for the tested triple subset, but not for every possible three-link combination. Extending exhaustive higher-order combination screening would be useful if the candidate set were reduced further or additional computational resources became available.

The present study also evaluates one AM-peak operating condition and does not explicitly model temporal variation across the day, weekday–weekend differences, incident conditions, seasonal demand, or long-term adaptation to new transfer facilities. Because the identified benefit is spatially localized, its magnitude may vary across time periods. Future work should therefore evaluate multiple temporal scenarios and, ideally, conduct before–after field validation following implementation of a candidate transfer intervention.

Finally, the selected link should be interpreted as a network-model recommendation rather than an immediate construction prescription. The optimization framework evaluates generalized passenger cost and spatial feasibility, but it does not fully account for detailed pedestrian design, accessibility standards, road-crossing safety, land ownership, station capacity, construction cost, institutional constraints, or implementation feasibility. These factors should be evaluated through site surveys and engineering assessment before any investment decision is made.

Despite these limitations, the corrected formulation provides a useful screening framework for identifying where an explicit Metro–BRT transfer connection is most likely to generate network benefit. Its main practical value is therefore in prioritization: rather than assuming that multiple interchange links should be implemented, planners can first identify whether individual candidate transfers produce measurable passenger benefits and whether additional links add marginal value.

For Isfahan, the corrected analysis supports prioritizing detailed field assessment of candidate 22 rather than automatically implementing a five-link intervention package. The next planning stage should examine pedestrian continuity, accessibility, crossing conditions, station-interface design, operational compatibility, and actual passenger transfer behavior around the selected location. If those site-level checks confirm feasibility, the candidate could then be evaluated through a pilot intervention or detailed engineering design.

From a methodological perspective, future research should focus less on adding further metaheuristic variants and more on strengthening the behavioral and empirical layers of the model. The largest potential improvements would come from observed OD/AFC data, calibrated route-choice parameters, dynamic transit assignment, measured service reliability and crowding, and locally validated environmental inputs. These additions would allow the optimization component to operate on a richer and more empirically grounded representation of passenger behavior.

Conclusions

This study developed and evaluated a corrected optimization framework for Metro–BRT transfer design in Isfahan by integrating a generalized-cost gravity model, a restricted multimodal passenger-network representation, explicit transfer-candidate screening, fixed-OD evaluation, and metaheuristic search. The principal methodological correction was to ensure that intermodal switching could occur only through explicitly activated Metro–BRT pedestrian transfer links and that the same OD matrix was retained across baseline and optimized designs. These changes remove two important sources of bias: implicit mode switching through shared network nodes and demand regeneration caused by recalculating OD flows after each network intervention.

The corrected candidate-generation and screening procedure produced 29 feasible Metro–BRT transfer alternatives within the adopted spatial and network-accessibility criteria. Individual evaluation showed that only two candidates generated a positive system-wide generalized-cost benefit. Candidate 22, connecting Metro node 10,000,008 to BRT node 20,000,059 through an approximately 249.2-m pedestrian transfer, produced the best result. Under the central fixed-OD formulation, total system generalized cost decreased from 6,265,519.636 to 6,258,241.797 passenger-min, corresponding to a reduction of 7,277.839 passenger-min or 0.116157%. The selected intervention improved 60 positive-demand OD pairs representing 5,790.238 demand units.

The combination analysis further demonstrated that additional transfer links did not improve the objective beyond the best single-link design. Exhaustive screening of all 406 candidate pairs produced no positive pairwise synergy, and targeted triple screening likewise yielded no incremental benefit over candidate 22 alone. These findings support the revised cardinality constraint $|S| \leq 5$ and a parsimonious design principle rather than imposing a fixed number of transfer facilities. In the corrected model, the preferred solution is therefore a single effective transfer connection rather than a compulsory multi-link intervention package. The algorithm comparison provides an additional consistency check. I-ACO, standard ACO, and deterministic greedy forward selection all identified candidate 22 and achieved the same optimized generalized cost. The three approaches differed mainly in computational effort, with the greedy method requiring fewer evaluations and shorter runtime in the fast benchmark. Consequently, the revised study does not claim numerical superiority of I-ACO. Instead, the agreement among distinct search procedures supports the stability of the selected solution within the corrected candidate set and objective formulation.

The gravity-model analysis was revised to avoid overstating empirical calibration. Because only an aggregate observed AM-peak BRT ridership value was available, βg could not be jointly estimated with total demand scale and the spatial OD pattern could not be independently validated. A central value of $\beta g = 0.05$ was therefore retained as an analytical assumption, while 0.005–0.20 was examined for demand-scaling sensitivity. The observed BRT count anchors aggregate demand magnitude only. The study does not claim full OD validation or invariance of the selected transfer across all plausible demand and service-parameter uncertainties.

From a planning perspective, the results indicate that the value of Metro–BRT integration in the studied network is spatially concentrated. The selected intervention generates a modest system-wide improvement but a clear benefit for a specific subset of OD movements. This distinction is important: the corrected result should be interpreted as a localized network-efficiency improvement rather than as evidence of a large system-wide transformation. Accordingly, candidate 22 should be regarded as a priority location for detailed field assessment,

including pedestrian accessibility, transfer safety, station-interface conditions, operational feasibility, and implementation cost.

The study also highlights an important methodological lesson for multimodal transport optimization. Reliable conclusions depend not only on the optimization algorithm but also on the realism of the network representation, the consistency of demand treatment, and the transparency of candidate generation and evaluation. In this case, correcting those modeling elements led to a smaller but more defensible benefit estimate and removed the need for strong claims regarding multiple transfer links, environmental improvements, or algorithmic superiority. Future research should therefore focus on strengthening the empirical and behavioral foundations of the model. Priority extensions include observed OD or AFC data, calibrated route-choice parameters, stochastic or schedule-based transit assignment, multi-period demand, measured reliability and crowding, validated fare and value-of-time information, and locally calibrated emission factors.

Overall, the revised framework provides a transparent and reproducible approach for screening and prioritizing Metro–BRT transfer interventions under limited data conditions. Its main contribution is not the magnitude of the reported improvement, but the combination of fixed-OD evaluation, restricted intermodal connectivity, explicit candidate screening, parsimonious network design, and cross-method consistency. These elements provide a more credible basis for subsequent engineering assessment and for future data-rich extensions of integrated public-transport network design.

Author contributions A.N. (Ali Naderan) supervised the project and provided guidance on methodology and data interpretation throughout the research. N.N. (Navid Nakhaie) conducted the research, collected and analyzed the data, and prepared the draft manuscript. S.A. (Shahriar Afandizadeh Zargari) supervised the project, developed the concept, provided guidance on methodology and reviewed the final draft. H.R (Hooman Rahimi) supervised the project, prepared data, analysis and discussions. All authors reviewed and approved the final manuscript.

Data availability The datasets used and/or analyzed during the current study available from the corresponding author on reasonable request.

Declarations

Competing interests The authors declare no competing interests.

Open Access This article is licensed under a Creative Commons Attribution 4.0 International License, which permits use, sharing, adaptation, distribution and reproduction in any medium or format, as long as you give appropriate credit to the original author(s) and the source, provide a link to the Creative Commons licence, and indicate if changes were made. The images or other third party material in this article are included in the article's Creative Commons licence, unless indicated otherwise in a credit line to the material. If material is not included in the article's Creative Commons licence and your intended use is not permitted by statutory regulation or exceeds the permitted use, you will need to obtain permission directly from the copyright holder. To view a copy of this licence, visit http://creativecommons.org/licenses/by/4.0/.

References

1. Reisi, M. et al. *Transport sustainability indicators for an enhanced urban transport data infrastructure* (Sustainable Cities and Society, Elsevier, 2020).
2. Nitwal, R. S. *A composite index for assessing sustainability of urban transportation systems* (Taylor & Francis journal on urban transport sustainability, 2025).
3. Ghafouri-Azar, M. et al. *The sustainable transport planning index: A tool for decision-making in public transport* (Sustainable Development (Wiley), 2023).
4. Chakhtoura, C. & Pojani, D. Indicator-based evaluation of sustainable transport plans: A case study of Paris *Trans. Policy*, (2016).
5. Nadi, P. A. et al. Review of methods and indicators in sustainable urban transport *J. Civil Sustain. Trans.*, (2017).
6. Khayamim, R. et al. A sustainable approach for selecting and timing urban transport projects *Sustain. Cities Soc.*, (2020).

7. Nnene, O. A. & co-authors. *Application of metaheuristic algorithms to the improvement of transit network design* (Journal of the South African Institution of Civil Engineering, 2017).
8. Haghshenas, H. et al. Sustainable transportation policies identification for a certain city using experiences of other similar cities: Case study Isfahan *Inter. J. Transportation Eng.*, (2015).
9. Mansourianfar, M. H. & Haghshenas, H. *Micro-scale sustainability assessment of transport infrastructure projects: Azadi district* (Isfahan. Cities, 2018).
10. Shayesteh, K. et al. Ecological impact assessment of the citizens of Isfahan's life using the ecological footprint index International *J. Adv. Life Sci.*, (2015).
11. Keshtkar, M. et al. Monitoring the ecological security of Esfahan with an ecological footprint approach *Geograph. Environ. Sustain.*, (2021).
12. Najafi, S. E. et al. *Ranking practicable technologies using TOPSIS, AHP and SAW: Case of Isfahan science and technology corridor* (Journal of Applied Research in Industrial Engineering, 2015).
13. Nnene, O. A. et al. *Transit network design with meta-heuristic algorithms and agent-based simulation* (IFAC-PapersOnLine, 2019).
14. Duran-Micco, J. et al. Transit network design considering link capacities using self-regulated ant colony optimization. Transportation Research Part B or D (hybrid airline / transport network). (2022).
15. Korzeń, M. *A two-step ant colony optimization approach for public transport infrastructure sections* (Archives of Civil Engineering, 2025).
16. Holliday, A. et al. *Learning heuristics for transit network design and scheduling* (Transportation Letters or similar TNDP-focused journal, 2025).
17. Shammas, M. I. et al. *Mitigating CO_2 emissions in African transport using decomposition analysis* (International Journal of Sustainable Transportation, 2024).
18. Owais, M. How to incorporate machine learning and microsimulation tools in travel demand forecasting in multi-modal networks. *Expert Syst. Appl.* **262**, 125563. https://doi.org/10.1016/j.eswa.2024.125563 (2025).
19. Owais, M., Ahmed, A. S., Moussa, G. S. & Khalil, A. A. Integrating underground line design with existing public transportation systems to increase transit network connectivity: Case study in Greater Cairo. *Expert Syst. Appl.* **167**, 114183. https://doi.org/10.1016/j.eswa.2020.114183 (2021).
20. Antczak, E. Quantification and assessment of sustainable urban mobility using composite indicators *Eur. J. Urban Stud.*, (2024).
21. Gudmundsson, H. et al. *Developing the Sustainable Urban Transport Index (SUTI)* (UNESCAP Transport and Communications Bulletin for Asia and the Pacific, 2017).
22. Velasco, A. & Gerike, R. A composite index for the evaluation of sustainability in Latin American public transport systems *Trans. Res. Part A*, (2024).
23. Salavati, A. & Haghshenas, H. Applying AHP and clustering approaches for public transportation decision-making: Case study of Isfahan city *Regional Trans. Plann. J.*, 2017).
24. Salavati, A., Nunes da Silva, F. & Haghshenas, H. Comparing public transport alternatives using AHP–TOPSIS and sustainability indicators: City of Isfahan. *Int. J. Transp. Eng.* **8** (1), 85–106 (2020).
25. GIS–ACO Sanandaj study. Transit network design using GIS and Ant Colony Optimization: Case of Sanandaj *J. Trans. Technol., c.* (2020).
26. Nayeem, M. A. et al. *Transit network design by genetic algorithm with elitism* (Transportation Research Part C (foundation for GA-based TNDP), 2014).
27. Asian Development Bank. Transport and Carbon Dioxide Emissions: Forecasts, Options Analysis, and Evaluation (ASIF-based project assessment manual). (2010).
28. Sporkmann, J. et al. Carbon emissions from European land transportation: An ASIF-based decomposition *Eur. Environ. Res. J.*, (2023).
29. n den Berg, M. et al. Current lifestyles in the context of future climate targets: ASIF decomposition tool for transport* *Environ. Res. Lett.*, (2021).
30. Recent A-S-I-F-E paper Electrification and modal shift in decarbonizing transportation: Extending the ASIF framework *Energy Convers. Manag.*, (2025).
31. Baabou, W. et al. *The ecological footprint of Mediterranean cities: Drivers and policy implications* (Ecological Indicators, 2017).
32. Antczak, E. & co-authors. &. Assessing sustainability of transport systems through indexes: A state-of-the-art review. (2024).

Publisher's note Springer Nature remains neutral with regard to jurisdictional claims in published maps and institutional affiliations.

Authors and Affiliations

Navid Nakhaie[1] · Ali Naderan[1] · Shahriar Afandizadeh Zargari[2] · Hooman Rahimi[3]

✉ Ali Naderan
Naderan@iau.ac.ir

[1] Department of Civil Engineering, SR.C, Islamic Azad University, Tehran, Iran

[2] School of Civil Engineering, Iran University of Science and Technology, Tehran, Iran

[3] Department of Civil Engineering, Islamic Azad University, Tehran, SQ.C, Iran